Proceedings of the ASME 2022 41st International Conference on Ocean, Offshore and Arctic Engineering
OMAE2022
June 5-10, 2022, Hamburg, Germany

OMAE2022-78924

NUMERICAL MODELLING OF DRAG AND LIFT FORCES ON AQUACULTURE NETS: COMPARING NEW NUMERICAL LOAD MODEL WITH PHYSICAL MODEL TEST RESULTS

Per Christian Endresen[1], Heidi Moe Føre
EXPOSED Aquaculture Research Centre
SINTEF Ocean
Trondheim, Norway

ABSTRACT

The Norwegian aquaculture industry expands towards sites with a harsher current and wave environment than before, while utilizing larger and more complex designs. This increases the need of precise modelling of hydrodynamic loads on nets to ensure a safe design that minimize risk of failure and avoids over-dimensioning and corresponding increase in costs. Established methods may overestimate drag forces, especially for high solidity nets.

In this paper, a new formulation for drag and lift forces on nylon multifilament aquaculture nets has been implemented in a numerical analysis software. The formulation was derived from towing tank tests of net panels with a wide range of solidities. The numerical code has been applied to estimate drag and lift forces on netting cylinders (representing a simplified, scaled net cage model) with four different solidities, similar to previously published physical model tests in a flume tank. The results from the numerical simulations and physical model tests were then compared to validate the new load model.

Resulting drag forces from the numerical simulations compared well with measured drag forces from the model tests, especially for the higher solidity netting materials, while numerical estimates of lift and measured total lift forces were dissimilar for some velocities and nets. Possible error-sources and uncertainties have been identified in both the numerical load model and physical tests.

A parameter study on the magnitude of drag and lift forces with varying net inclination angle was conducted and indicated that net panels and net cylinders may affect the flow differently. Applying formulas derived from net panel tests may therefore not be straightforward. The study also showed that the estimated total drag forces were dependent on the lift formula and vice versa, due to changes in net cage deformation.

Keywords: aquaculture, net cage, netting, solidity, drag force, drag coefficient, lift force, lift coefficient.

NOMENCALTURE

C_D	Drag coefficient
C_L	Lift coefficient
Sn_m	Netting solidity measured by image analysis
Sn	Estimated netting solidity
t	Netting twine thickness
s	Netting mesh side
r	Flow reduction factor
θ	Angle between net panel normal vector and incident flow vector
a_1	Parameter for drag force shape function
a_3	Parameter for drag force shape function
b_2	Parameter for lift force shape function
b_4	Parameter for lift force shape function
V	Relative velocity between net element and the undisturbed fluid flow. Uniform constant flow velocity in net cylinder tests
ρ	Density of fresh water
d	Bottom weight cylinder diameter
h	Bottom weight cylinder height

1. INTRODUCTION

As the Norwegian fish farming industry expands towards more exposed sites due to an increased demand for farmed fish and limited available sites in sheltered and near-shore areas, there is an even larger need for precise models for estimation of hydrodynamic loads on fish farms.

The nets enclosing the fish represent a large contribution to the total hydrodynamic excitation forces on traditional fish farms, thus accurate estimation of these forces is important. This is not only to prevent failure, possible fish escapes or risk to

[1] Contact author: Per.Christian.Endresen@sintef.no

human safety, but also to prevent over dimensioning which leads to increased production costs.

Model tests on net panels or net cages are often utilized to gain more knowledge of drag and lift forces acting on aquaculture nets. Data from several panel test and model tests of net cages are available [1 - 6]. In structural design, loads on high solidity nets are often of major interest. Several standards, like the Norwegian standards fish farms [7], requires that an increase in netting solidity due to biofouling should be accounted for in structural design. Established methods may overestimate drag forces for higher solidities [8, 9], and this has motivated the development of new load models for net structures. With this background, Moe Føre et al. [8, 9] performed towing tests on net panels, followed by the development of a new load model based on the panel tests and a new and improved method for determining netting solidity [9].

The netting solidity is the parameter that affects drag forces on nets the most and is therefore vital to estimate accurately. The solidity is defined as the ratio between the solid area (netting material) and the netting area. In practice, the solidity is often estimated based on manual measurements of twine thickness and mesh side, often estimated as Sn=2t/s, where t is the twine thickness and s are the mesh bar length, respectively. This approach may account for the extra material often found in the joints (knots) of the netting. This method often yields uncertain solidity estimates, as it is sensitive to subjective aspects such as how much the netting is compressed and stretched during measurements [9]. In addition, manual estimated does not consider the significant variations in twine thickness along the twine. Moe Føre et al. [9] showed that using image analysis with a standardized setup for acquiring pictures and analyzing them not only improved the accuracy of solidity estimates, but also improved the quality of drag force parametrization.

The work presented in this paper is a continuation of Moe Føre et al. [8, 9] and describes the implementation and testing of the new formula for hydrodynamic loads on aquaculture nets in a numerical code for time domain simulations of marine systems (FhSim, [10, 11]). The goal was to test the load model's performance with regards to estimating loads on aquaculture net cages.

2. MATERIALS AND METHODS

The new load model has been implemented in FhSim and validated by comparing the results with results from a state-of-the-art method for estimating hydrodynamic loads on aquaculture net cages by Kristiansen and Faltinsen [12], and model tests on netting cylinders in current performed by Moe-Føre et al. [13].

2.1 Net models

Moe-Føre et al. [13] conducted physical model tests on circular netting cylinders in a flume tank exposed to constant fluid velocities up to 0.93 m/s (MF2016). The netting cylinders were simplified representations of net cages, circular cylindrical in shape with straight walls, attached to a solid stationary steel ring at the top and with an open freely hanging bottom, i.e. no bottom cone.

Four netting cylinders from [13] were chosen and has been simulated in this work. The four nets had solidities of 0.19, 0.30, 0.35 and 0.43 and have been named N19, N30, N35 and N43, respectively. They all had the same diameter and height and 16 individual evenly spaced bottom weights at the bottom perimeter of the net. The net cylinder diameter was 1.75 m, while the height (in water with weights attached) where 1.55 m. The weights had a submerged weight of 5.15 N each. Relevant parameters for the four applied netting materials are given in Moe-Føre et al. [13] and presented in **Table 1**. A picture of net cylinder N35 from the experiments and a visual representation of the numerical discretization of the net in FhSim are shown in **Figure 1**.

Table 1: Netting material dimensions and parameters for all nets.

Parameter\Net	N19	N30	N35	N43
Netting mesh side [mm]	25.5	16.2	8.3	5.8
Netting twine thickness [mm]	2.42	2.35	1.41	1.35
Measured solidity (Sn_m) [-]	0.194	0.302	0.347	0.434
Estimated solidity (Sn=2t/s) [-]	0.190	0.290	0.340	0.466
Netting wet weight* [N]	4.222	6.267	4.403	5.777

**Estimated by FhSim*

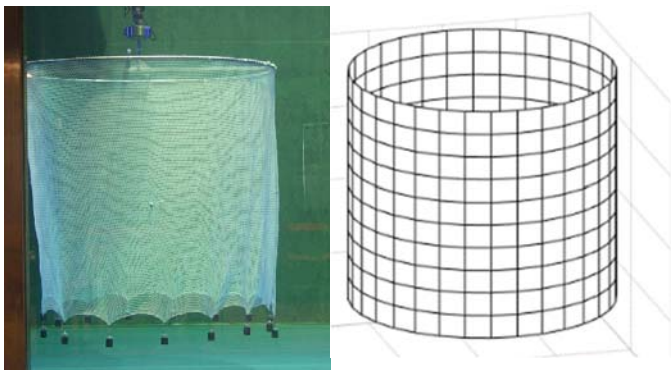

Figure 1: Picture from experiments (net N35) by (Moe-Føre et al. [13]) (left) and visual presentation of numerical discretization in FhSim (right).

2.2 Numerical modelling of net and hydrodynamic loads

The nets were modelled in FhSim, with properties according to **Table 1**. The nets were discretized into 32 elements along the circumference, and 10 over the height of the netting (**Figure 1**). A finer discretization of 64 times 20 elements were tested, but not applied, as it did not yield significantly improved calculations of forces and deformations.

The finite element structural model in FhSim [14] automatically divides each 4-sided element into 2 triangular elements to, among others, enable deformation and ensure that the three nodes of each element is in the same plane. This means that the numerical net model is comprised of 640 triangular net panels.

FhSim uses a water density of 1025 kg/m^3 for the calculation of weight in water, while the model tests were performed in fresh water (1000 kg/m^3). The netting material was given a density of 1165 kg/m^3, equal to the sum of the density of Nylon and the difference in density between fresh and seawater. This is a slightly high estimate according to Moe et al. [15, 16], as the netting twines are not solid but contains multiple Nylon fibers. A water density of 1000 kg/m^3 was applied in drag and lift force calculations.

The model by Kristiansen and Faltinsen [12] is based on solidity estimates (Sn=2t/s has been applied), while the new model by Moe Føre et al. [9] apply solidity-measurements from a manual image analysis (Sn_m, **Table 1**). The two hydrodynamic models are henceforth named MF2021 [9] and K&F2012 [12].

The numerical finite element model of the netting cylinder structure [14] and the relation between load coefficients and the element orientation to the fluid flow is the same for the two compared models. The differences between the two load models are found in the drag coefficient formulation for $\theta = 0°$ (flow perpendicular to the panel) and lift coefficient for $\theta = 45°$, and the flow reduction (wake effect) on the downstream part (half) of the net. θ is the angle between the panel normal vector and the flow velocity vector.

The elements orientation dependencies presented in K&F2012 have been applied in both models, where load coefficients as a function of inclination angle for each net element were formulated as follows [12]:

$$C_D(\theta) = C_D(\theta = 0) \cdot (a_1 \cos(\theta) + a_3 \cos(3\theta)) \quad (1)$$

$$C_L(\theta) = C_L(\theta = 45°) \cdot (b_2 \sin(2\theta) + b_4 \sin(4\theta)) \quad (2)$$

Note that the criterion $a_1 + a_3 = 1$ must be upheld to obtain the correct drag coefficient for $\theta = 0$, and $b_2 = 1$ to obtain the correct lift coefficient for $\theta = \pi/4$. In MF2021, drag and lift coefficients ($C_D(\theta = 0°)$ and $C_L(\theta = 45°)$, and the flow reduction factor (r) were given as:

$$C_D(\theta = 0°) = 1.782 \cdot Sn_m^2 + 1.057 \cdot Sn_m - 0.053 \quad (3)$$

$$C_L(\theta = 45°) = 1.693 \cdot Sn_m^2 - 0.217 \cdot Sn_m + 0.022 \quad (4)$$

$$r = 1.08 - 0.97 \cdot Sn_m \quad (5)$$

Sn_m is the netting solidity measured by image analysis. Drag and lift forces acting on each net element are then calculated as $0.5\rho C_{D,L} A V^2$ ($C_{D,L}$ from eq. 1 and eq. 2), where ρ is the water density, A is the circumscribed area of the net element and V is the relative velocity between the element and the fluid flow. The drag force will act in the direction of the relative fluid flow, while the lift force depending on net element orientation, may point in any direction perpendicular to the drag force. In these analyses, we apply a constant horizontal fluid flow, and V is thus equal to the fluid flow velocity when the simulation reaches a steady state, i.e. the drag force vector is horizontal for steady state. For the net cylinder, the drag force vector is horizontal in the same direction as the fluid flow velocity while lift is defined to be vertical with a positive direction upwards.

Specific values for a_3 and b_4 were chosen based on results from the towing tests that form a basis for MF2021. In the towing tests [9] the net panels were tested at $\theta = 0°$ and $\theta = 45°$, and resulting load coefficients were given. For a Reynolds number $Rn \cong 2000$, $a_3 = 0.065$ was found to estimate the expected drag coefficient for $\theta = 45°$ applying eq. 1. For the lift expression (eq. 2), $b_4 = 0.12$ were chosen based on towing test result with inclination angles (θ) equal to 0, 22.5, 45 and 67.5 presented in Moe Føre et al. [8]. These parameter values along with nominal values ($a_3 = b_4 = 0$) have been applied to investigate the effect of parameter variation when modelling drag and lift forces on the netting cylinders.

Table *2* gives an overview of model designations and parameter values that have been used in the simulations of the different net models (N19, N30, N35 and N43), while **Figure 2** presents normalized drag and lift coefficients (eq. 1 and eq. 2) for different a_1, a_3, b_2 and b_4 values. Essentially, **Figure 2** shows plots of the functions $a_1 \cos(\theta) + a_3 \cos(3\theta)$ and $b_2 \sin(2\theta) + b_4 \sin(4\theta)$ found in eq. 1 and eq. 2, respectively. It can be noted that the drag and lift coefficients presented in Moe Føre et al. [8] were based on manual solidity measurements (by use of slide caliper and ruler for the mesh twine and mesh bar measurements) and solidity estimated by Sn=2t/s. Further details of the load models can be found in Kristiansen and Faltinsen [12], Moe-Føre et al. [9] and a description of FhSim can be found in Reite et al. [10] and Su et al. [11].

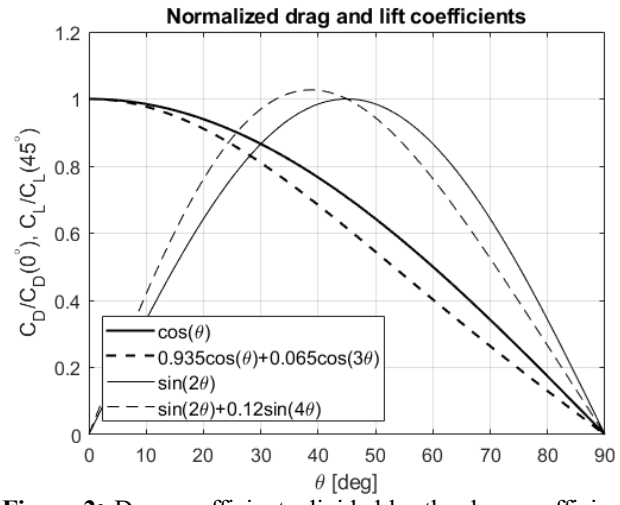

Figure 2: Drag coefficients divided by the drag coefficient for $\theta = 0°$ (cosine functions) and lift coefficients divided by the lift coefficient for $\theta = 45°$ (sine functions) for a net element. θ is the angle between the net element normal vector and flow direction.

Table 2: Model names and coefficients for the angel dependency of the drag- and lift coefficients.

Model\Parameter	a_1	a_3	b_2	b_4
MF2021, nominal	1	0	1	0
MF2021, a3=0.065	0.935	0.065	1	0
MF2021, a3=0.065 b4=0.12	0.935	0.065	1	0.12
MF2021, b4=0.12	1	0	1	0.12
K&F2012, nominal	1	0	1	0
K&F2012, a3=0.065 b4=0.12	0.935	0.065	1	0.12

2.3 Numerical modelling of bottom weights

To best be able to compare simulated results with the model tests in Moe-Føre et al. [13], modelling of the 16 individual bottom weights needed special consideration. For each node in the numerical netting model where a weight was attached, a horizontal force and a vertical force representing the drag forces acting on the weight and the submerged weight of the cylinder was applied. The drag force was calculated based on the given drag coefficient for the cylinders ($C_D \approx 1.1$), found by tests in Moe-Føre et al. [13]. The submerged weight of each weight cylinder (16 in total) was estimated and set to 5.15 N, based on reported dimensions of the steel cylinders in [13]. The drag force on each weight cylinder was modelled as $F_D = 0.5\rho C_D dhV^2$, where ρ is the density of fresh water (1000 kg/m^3), C_D is the drag coefficient (1.1), d and h are the diameter (4 cm) and height (6 cm) of the cylinder and V is the flow velocity (**Table 3**).

Table 3: Estimated drag force on each of the 16 individual cylindrical weights and total drag force for all weights.

Velocity [ms^{-1}]	0.12	0.26	0.39	0.50	0.65	0.76	0.93
F_D individual [N]	0.019	0.089	0.201	0.330	0.558	0.762	1.142
F_D^{total} total [N]	0.30	1.43	3.21	5.28	8.92	12.20	18.27

2.4 Presentation of drag and lift forces

The results presented in this document are the total hydrodynamic drag and lift forces acting on the netting cylinder only, as calculated by FhSim. For the lift forces this is equal to the difference in measured vertical retention force between the applied velocity and 0 m/s at the fixed upper circumference of the netting cylinder. For the drag forces this is equal to the difference in corresponding horizontal retention force when the applied drag forces from the weight cylinders are subtracted. In FhSim the drag at 0 m/s is 0 N, while the vertical force at the top connection includes the submerged weight of both the net and the weight cylinders for all velocities.

3. RESULTS AND DISCUSSION

Figure 3 through **Figure 6** show drag and lift forces on the nets simulated with the two different models (MF2021 and K&F2012) compared with results from the physical model tests MF2016. A variation in parameters describing the angle dependency for drag and lift (**Figure 2**) has also been performed, and results are shown in the figures. The performance of the models, how they react to changes in angle dependency parameters and what that may imply, possible error sources along with suggestions for improvements have been discussed.

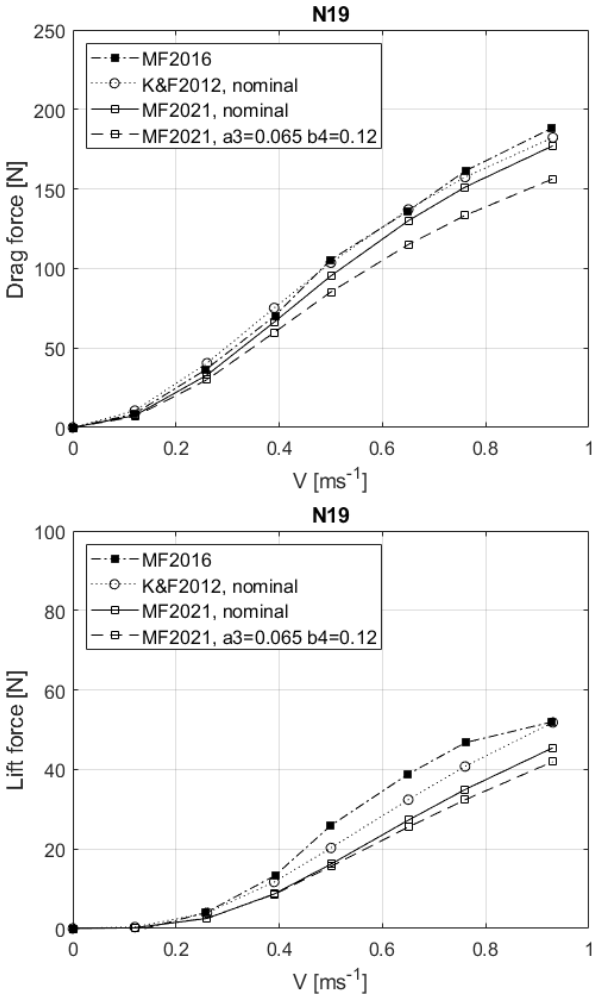

Figure 3: Drag and lift forces for net N19. Results from experiments (MF2016/[13]) compared with estimated drag and lift forces from numerical simulations (K&F2012/[12], MF2021/[9]).

3.1 Drag and lift forces with nominal parameter values

Comparison between FhSim simulations and the model tests shows that for load model MF2021, nominal values for a_1, a_3, b_2 and b_4 ("MF2021, nominal",

Table 2) on average gave results closest to the measured drag forces for all nets. For the drag forces, considering all four nets, MF2021 compared well with experiments from a fluid velocity of 0.26 m/s to 0.93 m/s (**Figure 7**). The best fit between numerical and experimental results was seen for velocities of 0.5 m/s and higher. For 0.5 m/s and higher simulation results for net N30, N35 and N43 were similar to experiment results, while the estimated drag forces for net N19 were somewhat lower than in the experiments (**Figure 7**). For the lift forces the results compared with experiments were more varied. For velocities of

0.26 m/s and higher net N35 and N43 compared well with experiments, while simulation results for net N19 were noticeable lower than lift forces measured in the experiments for all velocities (**Figure 7**). Comparison between simulated lift and results from experiments for net N30 was more varied than for the other nets. The occasional large discrepancies between measured and estimated drag and lift loads seen in **Figure 7** and **Figure 8** may be explained by the fact that uncertainties and error sources may have a relative large effect on the low loads found at low velocities. This is further discussed in chapter 3.4 and in [13].

For the model "K&F2012, nominal" the drag forces were on average higher than the experiment results for net N30, N35 and N43 (**Figure 8**). The largest relative difference was seen for N43 and the second highest flow velocity (0.76 m/s) if the two lowest velocities are disregarded. Drag forces estimated with "K&F2012, nominal" compared well with experiments for net N19, especially for velocities of 0.5 m/s to 0.93 m/s. Comparison between lift forces simulated with "K&F2012, nominal" and lift forces from experiments were, as for "MF2021", varied. For 0.5 m/s and higher the simulated lift forces were lower than lift forces measured in the experiments for N19, N35 and N43, with the exception of lift for N19 and N43 for 0.93 m/s, which were similar to the values found in the experiments. The comparison of lift for N30 were varied for velocities lower than 0.5 m/s, and simulated lift was higher than what was observed in the experiments with an increasing trend for 0.5 m/s and higher.

3.2 Parameter study: angle dependency

A detailed parameter study with load model MF2021 was performed on net N35 (**Figure 5**). Parameters determining drag and lift force on each net element in the numerical net model was varied according to

Table *2*. "MF2021, $a_3 = 0.065$" resulted in a decreased drag force while increasing the lift force (all velocities) compared with "MF2021, nominal". "MF2021, $b_4 = 0.12$" increased the drag force while reducing the lift force compared with nominal parameter values. Setting $a_3 = 0.065$ and $b_4 = 0.12$ ("MF2021, $a_3 = 0.065$ $b_4 = 0.12$") resulted in a decrease in drag and lift compared to nominal values for all flow velocities. This was also the case for load model "K&F2012, $a_3 = 0.065$ $b_4 = 0.12$", were drag and lift forces were reduced compared to nominal parameter values.

"MF2021, $a_3 = 0.065$ $b_4 = 0.12$" gave higher drag forces than "MF2021, $a_3 = 0.065$" for 0.5 m/s flow velocity and higher, but lower drag forces than "MF2021, nominal" for all velocities. For a flow velocity of 0.39 m/s and lower the drag forces for "MF2012, $a_3 = 0.065$ $b_4 = 0.12$" and "MF2021, $a_3 = 0.065$ " are similar. " MF2021, $b_4 = 0.12$" gave the highest estimated drag forces of all tested parameter values for MF2021. For lift however, the highest forces are predicted by " MF2021, $a_3 = 0.065$ ", followed by " MF2021, nominal", "MF2021 $a_3 = 0.065$ $b_4 = 0.12$" and " MF2021, $b_4 = 0.12$".

"MF2021, $a_3 = 0.065$ $b_4 = 0.12$" was also used to estimate forces on net N19 (**Figure 3**). For net N19 the estimated drag forces were lower than "MF2021, nominal" for all velocities, while the lift forces were lower than estimated with nominal parameter values for 0.39 m/s to 0.93 m/s.

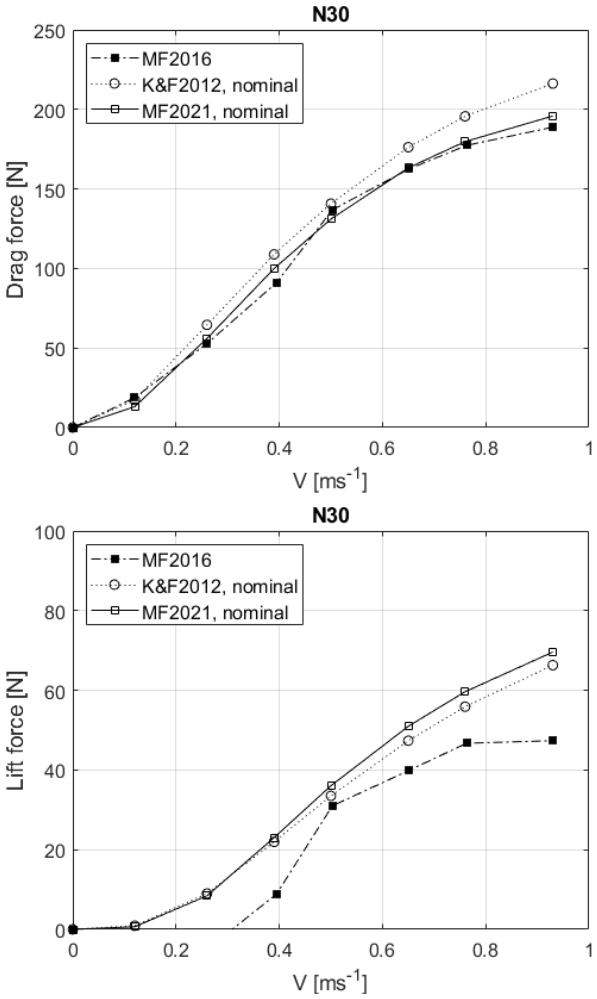

Figure 4: Drag and lift forces for net N30. Results from experiments (MF2016/[13]) compared with estimated drag and lift forces from numerical simulations (K&F2012/[12], MF2021/[9]).

Since the implementation of the angle dependency don't affect the drag coefficient for $\theta = 0°$ and lift coefficient for $\theta = 45°$ for the net elements, the drag and lift forces for net cylinders N30 and N43 may be similarly affected by parameter variations as net cylinders N19 and N35.

Since the implementation of the angle dependency also is independent of load model (MF2021 or K&F2012), it may be that a_1, a_3, b_2 and b_4 equal to 0.935, 0.065, 1 and 0.12 for K&F2021 would lead to a smaller difference between simulated drag forces and drag forces from experiments for nets N30 and N43 as well as N35. For net N19 it may lead to simulated drag forces being lower than found in the experiments. The lift forces may decrease for all nets compared with nominal values.

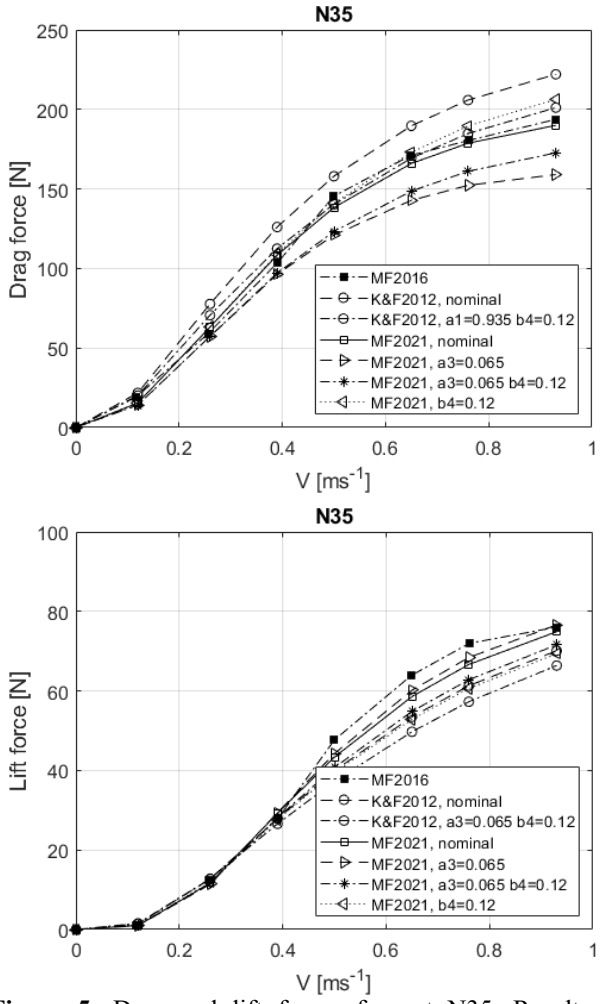

Figure 5: Drag and lift forces for net N35. Results from experiments (MF2016/[13]) compared with estimated drag and lift forces from numerical simulations (K&F2012/[12], MF2021/[9]).

One explanation for the observed results of parameter change is the associated effect on drag and lift force on individual net elements and the consequent change of net cylinder deformation, which in turn affects the loads on the net cylinder. The effect of changing parameter values on loads and net deformations are complicated. An explanation, with simplified examples for the observed behavior, will in the following be given.

When $a_3 > 0$ (without changing other parameters), the drag force estimated for each net panel decreases (compared to nominal) for all orientations except perpendicular and parallel. This may lead to reduced overall deformation of the net cylinder. The total lift force may then, if b_4 is kept at nominal values, for some levels of deformations increase compared with a simulation where drag and lift coefficients were nominal, due to changes in panel orientations to the fluid flow. As an example, we consider a panel with orientation angle $\theta > 45°$. Any reduction in orientation angle θ, as long as θ is not reduced below 45°, will result in an increased estimated lift on that panel (valid for $b_4 = 0$, see **Figure 2**). This may in total for the entire net cylinder result in an increased total lift force while at the same time the estimated total drag forces are reduced.

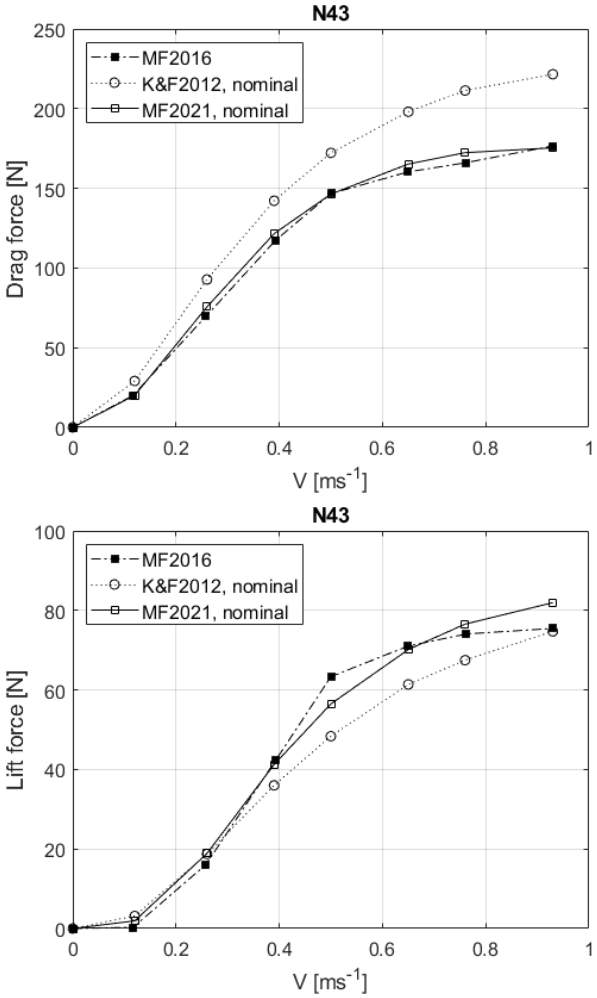

Figure 6: Drag and lift forces for net N43. Results from experiments (MF2016/[13]) compared with estimated drag and lift forces from numerical simulations (K&F2012/[12], MF2021/[9]).

If $b_4 > 0$ the lift curve in **Figure 2** will shift towards the left. Compared with nominal values, $b_4 = 0.12$ will result in lower lift forces on a panel for orientation angles θ larger than 45° and an increase in the lift force for θ smaller than 45°. For $b_4 > 0$ and $a_3 = 0$, dependent on the situation, this may lead to a reduction in total lift forces compared with nominal parameter values, resulting in less deformation. This, in turn, will result in an increase in the total drag forces since the drag force for each net panel (as modelled) continuously increase with decreasing θ values.

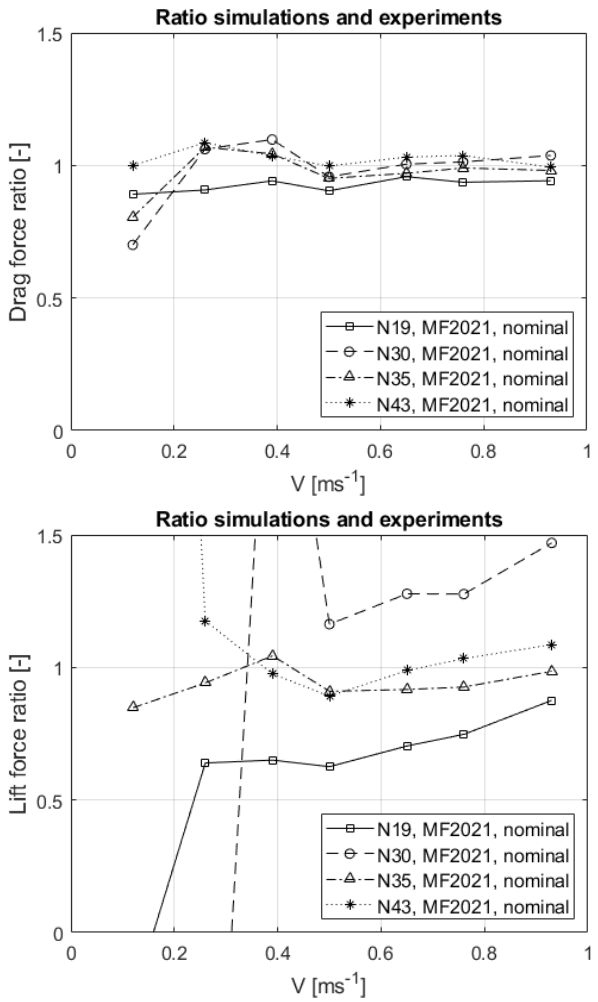

Figure 7: Drag and lift force ratio between numerical simulations (MF2021/[9]) and experiments (MF2016/[13]) for all nets.

The effects of varying a_3 and b_4 cannot, as indicated above be treated separately without considering the consequent change in deformations, as a decrease in for instance total drag may result in an increase in total lift, which in turn affects the overall deformations and to some degree may negate the effect on deformation of decreased drag due to an increase in a_3. A similar argument can also be used if we increase b_4 while keeping a_3 constant. The lift may decrease resulting in less overall deformations, which in turn increase the drag forces due to a change in the panels orientations to the fluid flow.

Although the chosen non-nominal parameter values ($a_3 = 0.065$ and $b_4 = 0.12$) was derived from results from model tests [8, 9], further investigation is needed to confirm these parameter values. The simulation results given in this paper indicate that nominal values (

Table *2*) give the best fit to the model test data for the model "MF2021". Setting a_1, a_3, b_2 and b_4 to 0.935, 0.065, 1 and 0.12 results in both lower drag and lower lift forces on the netting cylinders compared with the model tests (simulated and tested for N19 and N35, see **Figure 3** and **Figure 5**).

Kristiansen and Faltinsen [12] indicate, according to their findings and load model, that both a_3 and b_4 should be larger than 0, and that the values for a_3 and b_4 probably will increase with increasing netting solidity. They did not find a clear relationship between netting solidity and parameter values.

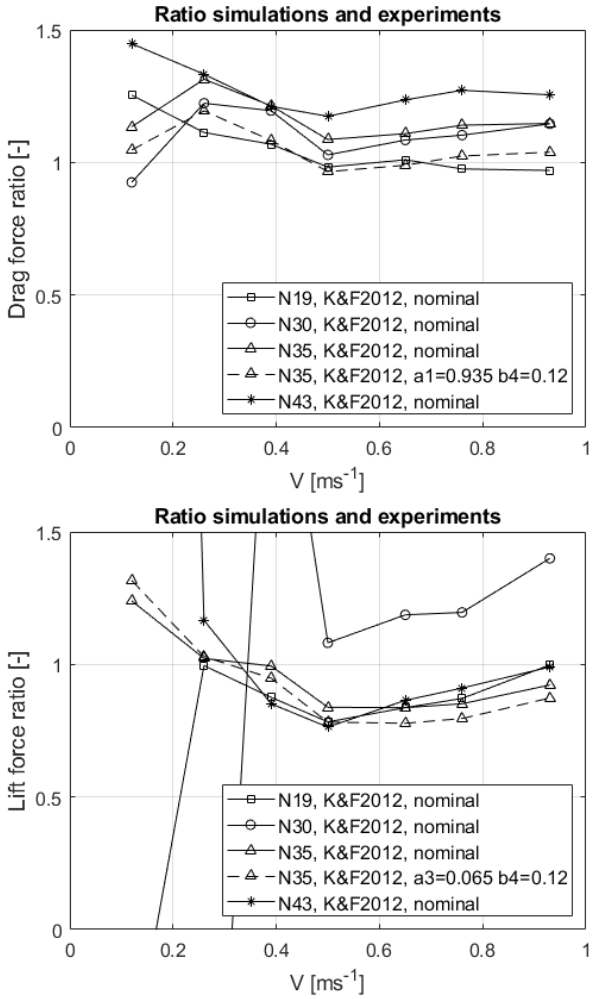

Figure 8: Drag and lift force ratio between numerical simulations (K&F2012/[12]) and experiments (MF2016/[13]) for all nets.

In the present paper, the goal was to investigate the performance of the load model from Moe Føre et al. [9]. Of the parameter variations in

Table *2*, "MF2021, nominal" displayed the best fit to the test data for all nets, with small variations in
the comparison of drag forces between the numerical model and experiment results (**Figure 7**).

This being said, it is possible that the angle dependency for physical nets is not equal between nets and may vary depending

on netting solidity and local netting geometry. Local netting geometry (twines and knots) is thought to impact the lift forces [9]. As the comparison between test results and simulations (MF2021, nominal) were close for all nets, it may also be that the variation in parameters is small. How the drag coefficient for $\theta = 0$ is estimated may also affect what is appropriate values for a_1, a_3, b_2 and b_4. However, both the statement that angle dependency may vary, and that the local geometry may affect lift needs further investigation.

3.3 Net cylinder deformation

A net cylinder may affect the fluid flow differently than a net panel. The possible difference in inflow conditions to the net for a net cylinder compared with a single net panel may be one explanation for why nominal parameter values, and not the values estimated from panel tests, give the best fit to experimental values for the net cylinders. More knowledge is needed on how the inflow conditions are affected by the net. The wake effect on the downstream parts of the net may also not be uniform in the model tests, as is modelled in FhSim.

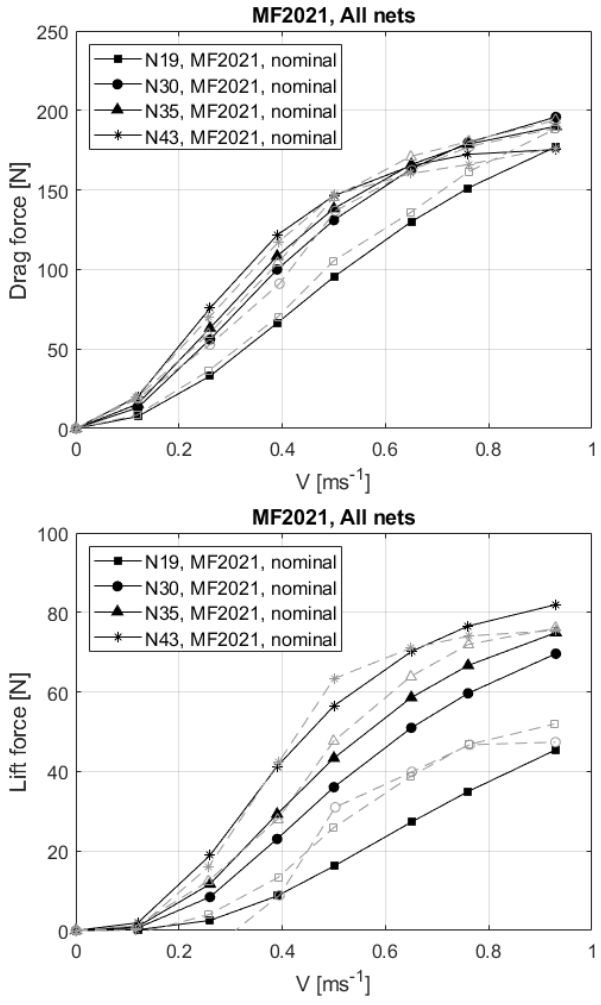

Figure 9: Estimated drag and lift forces from numerical simulations (MF2021/[9]) for all nets. Grey markers and lines represent the results from experiments (MF2016/[13]).

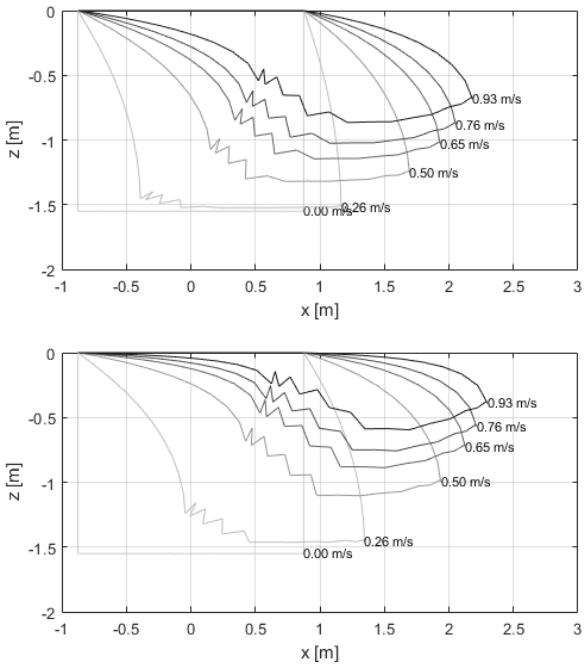

Figure 10: Side view of deformation from FhSim of centerline (side walls) and bottom perimeter of net cylinders for fluid velocities from 0 m/s to 0.93 m/s. Top: N19. Bottom: N35. Model: MF2021/[9], nominal.

Figure 9 shows drag and lift forces (FhSim, MF2021, nominal) on the four different nets compared with test results from Moe-Føre et al. [13]. The simulation results indicates that for velocities up to 0.5 m/s an increase in solidity leads to an increase in drag forces on the netting cylinders. For velocities above 0.6 m/s, the estimated drag loads tend to be less dependent on solidity. The exception (FhSim simulations) is N19, which has the lowest drag forces for all velocities, except for 0.93 m/s where the drag force for N19 is approximately equal to the drag force for N43. Similar, but not equal relations were observed for the model tests presented in Moe-Føre et al. [13], which may be due to fluid-structure interaction effects for highly deformed models. This is discussed in Moe-Føre et al. [13].

The lift, however, increase with increasing velocities for all solidities simulated in FhSim. The model tests of the net cylinders show a general increase in lift with increased solidity, but the relation is not as clear as in the FhSim simulations. The reduction in total drag forces with increasing solidity for the two highest velocities (FhSim, "MF2021, nominal") may be due to increased deformations causing the net to approach the limits for possible deformation (net cylinder approaching a compressed and flat form).

Figure 10 shows deformations (FhSim, MF2021, nominal) of the net centerline for net N19 and N35, respectively. The

figure illustrates simulated deformations for 0, 0.5 and 0.93 m/s, for which N35 has larger deformations than N19. An increase in the netting solidity may result in the net cylinder approaching its limits for possible deformations sooner (lower velocities), and may partly explain why simulations (MF2021, nominal) show larger drag forces for N30 and N35 compared to N43 for the two highest velocities.

The plot of centerline displacement also indicates how the net is folded on the upstream side. This effect is also seen in the model tests Moe-Føre et al. [13], shown in **Figure 11**. Here, a perspective view of the deformations of net N35 (FhSim, "MF2021, nominal") are placed over a picture from the model tests (only the foremost half of the net from FhSim is shown). This figure is meant to give a visual indication of how the simulated deformation compares to the model tests. Differences in viewing angle and distance as well as camera properties may affect the comparison.

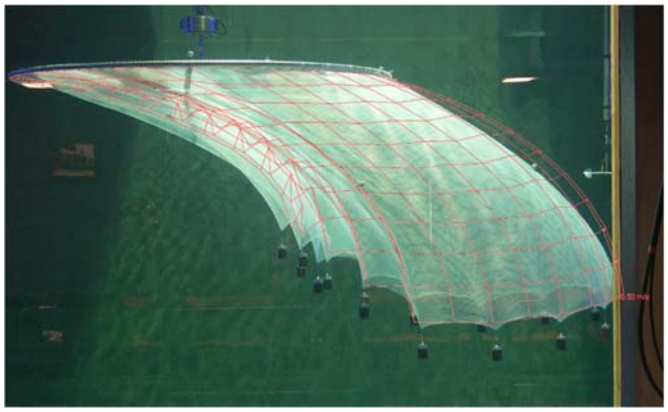

Figure 11: Picture from experiments Moe-Føre et al. [13] overlayed with perspective view of deformations estimated with "MF2021/[9], nominal". Net: N35. V=0.5 m/s.

3.4 Uncertainties and error sources

There are several possible uncertainties and error sources which may affect either the results from the numerical simulations or the results from the model tests and hence affect the comparison between the two. There may be errors in the model tests setup, i.e. inaccuracies in the physical model (size and weight). Solidity measurements may induce errors. Pictures and image analysis where at the time done manually. There might also be uncertainties in force measurements, which is thought to be more likely for lower velocities. Possible angle deviance from horizontal of the steel ring and load censor may have caused the measurement of negative total lift at low velocities for some of the nets. Inaccuracies in the netting and skew netting may have put strains on the net and hence caused tensions that affect the deformation and hence the forces.

The mentioned possible error sources focus on the tested model and measurements. The numerical code may also contain sources for error, such as for instance structural modelling and the values used for mechanical properties of the netting. The chosen value for netting density may deviate slightly from what was tested and hence also affect the comparison. In addition, there is the load model and choice of constant angle dependency parameters (

Table 2). This might affect the deformation and hence also the total forces. The chosen load model (MF2021) is intended for relatively high Reynolds numbers, as these are interesting in structural design.

4. CONCLUSION

Drag forces estimated by the numerical code when using the load model from Moe Føre et al. [9] (MF2021, nominal) compared well with results from model tests [13]. There were larger differences between simulated lift forces and lift forces measured in the experiments. The results indicate that the simulated drag forces on a net cylinder are dependent on the lift force formulation and vice versa.

ACKNOWLEDGEMENTS

The research has been funded by the Research Council of Norway, through the "EXPOSED Aquaculture Research Centre", with grant number 237790. We would also like to thank the partners of EXPOSED for good cooperation during the project.

REFERENCES

[1] Rudi, H., Løland, G. and Furunes, I., 1989. Modellforsøk med nøter. Krefter og gjennomstrømning på enkeltpaneler og merdsystemer. SINTEF Report, Trondheim, Norway. 1989.

[2] Løland, G., 1991. Current forces on and flow through fish farms. PhD thesis, Norwegian Institute of Technology, Division of Marine Hydrodynamics, Trondheim. 1991.

[3] Zhan, J.M., Jia, X.P., Li, Y.S., Sun, M.G., Guo, G.X., Hu, Y.Z., 2006. Analytical and experimental investigation of drag on nets of fish cages. Aquacultural Engineering, Volume 35, Issue 1, Pages 91-101. 2006. ISSN 144-8609. https://doi.org/10.1016/j.aquaeng.2005.08.013.

[4] Balash, C., Colbourne, B., Bose, N., Raman-Nair, W., 2009. Aquaculture Net Drag Force and Added Mass. Aquacultural Engineering, Volume 41, Issue 1, Pages 14-21. 2009. ISSN 0144-8609. https://doi.org/10.1016/j.aquaeng.2009.04.003.

[5] Patursson, Ø., Robinson Swift, M., Tsukrov, I., Simonsen, K., Baldwin, K., Fredriksson, D. W., Celikkol, B., 2010. Development of a porous media model with application to flow through and around a net panel. Ocean Engineering, Volume 37, Issues 2–3, Pages 314-324. 2010. ISSN 0029-8018. https://doi.org/10.1016/j.oceaneng.2009.10.001

[6] Gansel, L. C., Jensen, Ø., Lien, E., and Endresen, P. C., 2014. Forces on Nets With Bending Stiffness-An Experimental Study on the Effects of Flow Speed and Angle of Attack. ASME. J. Offshore Mech. Arct. Eng. November 2014. https://doi.org/10.1115/1.4027954.

[7] NS 9415.E:2009. Marine fish farms - Requirements for site survey, risk analyses, design, dimensioning, production, installation and operation. Standards Norway. 2009.

[8] Moe Føre, H., Endresen, P.C., Norvik, C., Lader, P., 2021. Hydrodynamic loads on net panels with different solidities. J. Offshore Mech. Arct. Eng. October 2021, Vol. 143 / 051901-1. DOI: 10.1115/1.4049723.

[9] Moe Føre, H., Endresen, P. C., and Bjelland, H. V., 2022. Load coefficients and dimensions of Raschel knitted netting materials in fish farms, ASME. J. Offshore Mech. Arct. Eng. August 2022; 144(4): 041301. https://doi.org/10.1115/1.4053698

[10] Reite, K.J., Føre, M., Aarsæther, K.G., Jensen, J., Rundtop, P., Kyllingstad, L.T., Endresen, P.C., Kristiansen, D., Johansen, V., & Fredheim, A., 2014. "FHSIM — Time Domain Simulation of Marine Systems." Proceedings of the ASME 2014 33rd International Conference on Ocean, Offshore and Arctic Engineering. Volume 8A: Ocean Engineering. San Francisco, California, USA. June 8–13, 2014. V08AT06A014. ASME. https://doi.org/10.1115/OMAE2014-23165

[11] Su, B., Reite, K.J., Føre, M., Aarsæther, K.G., Alver, M.O., Endresen, P.C., Kristiansen, D., Haugen, J., Caharija, W., & Tsarau, A., 2019. "A Multipurpose Framework for Modelling and Simulation of Marine Aquaculture Systems." Proceedings of the ASME 2019 38th International Conference on Ocean, Offshore and Arctic Engineering. Volume 6: Ocean Space Utilization. Glasgow, Scotland, UK. June 9–14, 2019. V006T05A002. ASME. https://doi.org/10.1115/OMAE2019-95414

[12] Kristiansen, T. and Faltinsen, O. M., 2012. Modelling of current loads on aquaculture net cages, Journal of Fluids and Structures, vol. 34, pp. 218–235, Oct. 2012, doi: 10.1016/j.jfluidstructs.2012.04.001.

[13] Moe-Føre, H., Lader, P. F., Lien, E., and Hopperstad, O. S., 2016. Structural response of high solidity net cage models in uniform flow, Journal of Fluids and Structures, vol. 65, pp. 180–195, Aug. 2016, doi: 10.1016/j.jfluidstructs.2016.05.013.

[14] Priour, D., 1999. Calculation of net shapes by the finite element method with triangular elements, Communications in Numerical Methods in Engineering, 15, pp. 755–763.

[15] Moe, H., Olsen, A., Hopperstad, O.S., Jensen, Ø., Fredheim, A., 2007. Tensile properties for netting materials used in aquaculture net cages, Aquacultural Engineering, Volume 37, Issue 3, 2007, Pages 252-265, ISSN 0144-8609, https://doi.org/10.1016/j.aquaeng.2007.08.001.

[16] Moe, H., Fredheim, A., Hopperstad, O.S., 2010. Structural analysis of aquaculture net cages in current, Journal of Fluids and Structures, Volume 26, Issue 3, 2010, Pages 503-516, ISSN 0889-9746, https://doi.org/10.1016/j.jfluidstructs.2010.01.007.